Preprint
UCRL-JC-135879

Flow Patterns Around a Complex Building

R. Calhoun, S. Chan, R. Lee, J. Leone, J. Shinn and D. Stevens

This article was submitted to
American Meteorological Society
11th Symposium on Global Change Studies
Long Beach, CA
January 9-14, 2000

September 24, 1999

U.S. Department of Energy

Lawrence
Livermore
National
Laboratory

4A.4 FLOW PATTERNS AROUND A COMPLEX BUILDING

R. Calhoun, S. Chan, R. Lee, J. Leone, J. Shinn, D. Stevens

Lawrence Livermore National Laboratory
7000 East Ave, Livermore CA 94550

1. INTRODUCTION

We compare the results of a computer simulated flow field around building 170 (B170) at Lawrence Livermore National Laboratory (LLNL) with field measurements. In order to aid in the setup of the field experiments, the simulations were performed first. B170 was chosen because of its architectural complexity and because a relatively simple fetch exists upwind (a field lies southwest of the site). Figure 1 shows a computational model of the building which retains the major architectural features of the real building (e.g., courtyard, alcoves, and a multi-level roof).

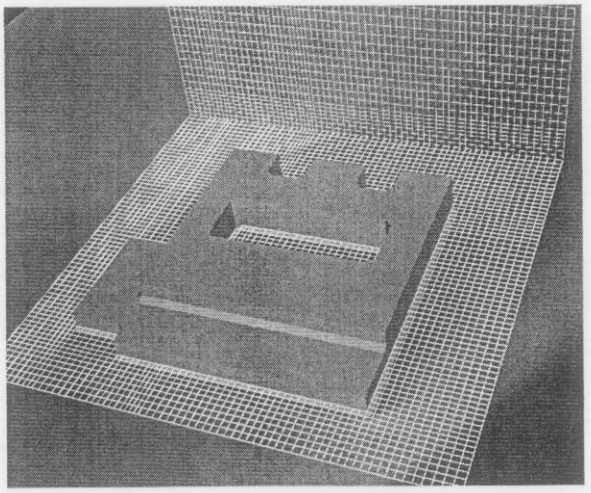

Figure 1. Mesh in the vicinity of B170.

Several important characteristics of the cases presented here are: 1) the flow was assumed neutral and no heat flux was imposed at the ground, representing cloudy or morning conditions, 2) a simple canopy parameterization was used to model the effect of a large row of eucalyptus trees which is located to the northeast of the building, 3) the wind directions studied were 200, 225, 250 degrees measured clockwise from true north (the prevailing winds at LLNL are from the southwest in the summer), 4) the incoming wind profile was modeled as logarithmic with a maximum of about 3 meters per second. In addition, note that the building is rotated counterclockwise by 25 degrees with respect to the east/west axis. For convenience, the flow is modeled in a coordinate system that has been rotated with the building (see Figure 2).

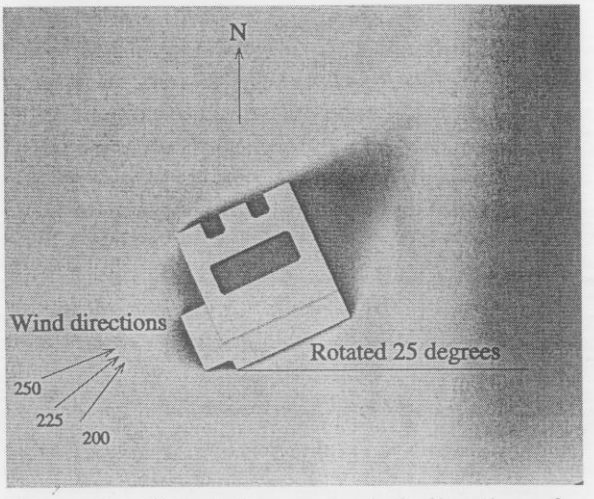

Figure 2. Orientation and wind directions for B170 wind flow study.

2. METHOD AND DOMAIN

The computational fluid dynamics code utilizes a finite element methodology (Chan, 1994) and has been adapted for use on massively parallel computer platforms (Stevens et al., 1999) via MPI (Message Passing Inteface). The simulations performed here used 128 processors of the ASCI Blue-Pacific machine. Approximately one million grid points were used in the computational mesh. The computational domain spans 400 x 400 x 80 meters, where the smaller dimension is in the vertical direction. A variety of different turbulent closures have been implemented and are available in the massively parallel code (see, for example, Gresho and Chan, 1998) Canopy effects are modeled with a simple drag term added to the momentum equations (Arya, 1988).

3. FIELD EXPERIMENT

The experimental arrangement is composed of an energy budget station, an array of sonic

anemometers, a sodar, and data from a nearby meteorological tower. The energy budget station sits upwind of the building in a field and measures wind speed/direction, incoming solar radiation, soil heat flux, and sensible heat flux. The sodar is placed on top of B170 and obtains vertical profiles of wind speed.

The sonic anemometers are mobile and are placed in key locations off a face of the building to gather data continuously for a number of days. The array is then moved to another side of the building to again gather data. A database is then built which may be queried to obtain a composite picture of the flow for specified flow conditions. For example, one may query the database to obtain only the data for strong winds which come from the 220-230 degree directions. As in the above exampe, the experimental data presented here for a given wind is actually a small range of values. In the following, we compare ranges of experimental data which are the closest available to the model wind directions (simulated before the experiment). The focus of the current level of experimental data is to characterize flow patterns on the 2.6m high horizontal plane.

4. FLOW FEATURES

The prominent features of the flow field are: 1) an asymmetric, tear-shaped recirculation zone behind the building, 2) a large region of reduced flow in the trees, 3) lid driven cavity-like flow in the courtyard with an additional helical pattern moving toward and exiting the northeast corner of the courtyard (for the wind directions 200 and 225), 4) a region of increased flow velocities and strong gradients between the southeast corner of the building and the row of trees, 5) air at a lower level in the recirculation zone enters the alcoves along the northern outer border of the building and exits at a higher level to be washed downstream for wind directions 200 and 225; for the 250 degree wind direction, there is an additional clockwise flow pattern looking aerially at the alcoves, and 6) weak reverse flow along the eastern edge of the building (for all wind directions).

4.1 Recirculation zone

The following two paragraphs discuss model predictions and then field results for the character of the recirculation at approximately the 2.6 meter height.

The general features of the (model) recirculation zone may be seen in Figure 3 and Figure 11 for the 200 degree case. At the 2.6 meter height, the tear-shaped region of momentum deficit extends downstream mainly from the northern and eastern sides of the building roughly 1.5 building widths before momentum values reach fifty percent of the free stream momentum. The recirculating region at the 2.6 meter height extends downstream less one half of the building width. At the 2.6 meter height, a mean eddy, rotating clockwise, is located near the northwest corner. Another mean recirculation eddy is located on the east side near the north corner and rotates counter clockwise. This can be seen more clearly in Figure 11 as a flattened mean recirculation on the east face of the building.

The experimental data in Figure 4 also shows evidence of a clockwise recirculation near the northwest corner of the building. There is also strong evidence of a counterclockwise recirculation on the eastern (north corner) of the building. These patterns are consistent with the model predictions of westerly flow along the northern face of the building and southerly flow along the eastern face (for 200 degree case).

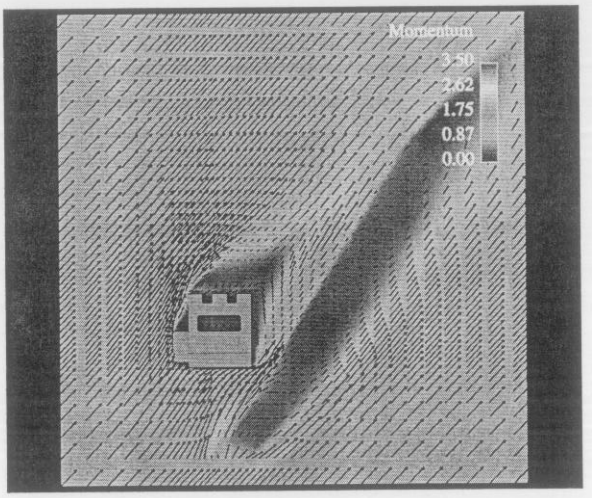

Figure 3. Velocity vectors and contours of momentum on a plane 2.6 meters above the ground. Wind direction: 200 degrees. See Figure 11 for magnified view of recirculation region.

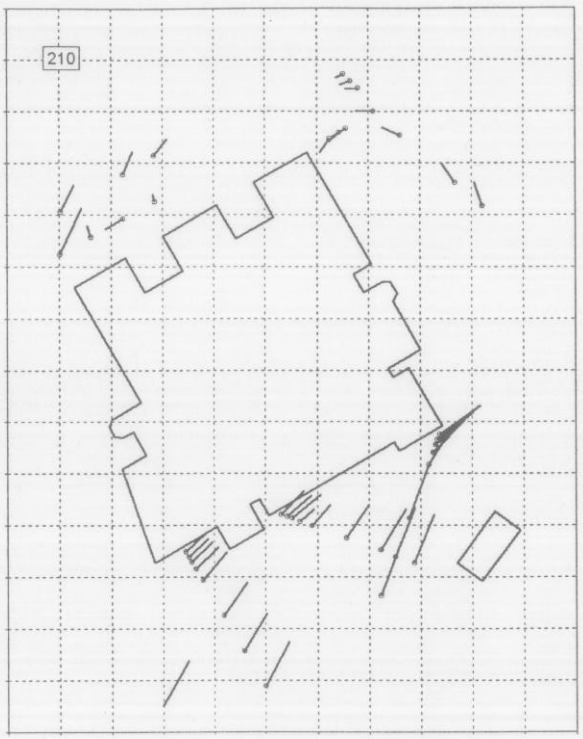

Figure 4. Experimental winds for 210 degrees. Tail of vectors indicated by circles.

Releases of lines of massless marker particles (representing small parcels of air) were used to gain an additional understanding of the modeled flow field. Releases along a diagonal behind the building at a level of 1 meter show that parcels of air which start in the recirculation zone are pulled closer to the building, into the alcoves, and finally move downstream, usually at an increased height. Releases from lines upstream of the building (at 1, 2, and 3 meters above the ground) show that several of the marker particles from the 3 meter height are likely to enter the recirculation zone and the courtyard while releases from the lower levels do not enter the courtyard (for the 200 degree case).

Figures 5, 6, 7, and 8 show how changes in wind direction impact downwind recirculations. In both the model predictions and the experimental data, the recirculation zone near the northwest corner flattens and finally disappears with increasingly westerly winds. Both the model predictions and experimental data agree that the recirculation on the eastern side near the north corner shifts directions; rotating counterclockwise with 200 and 225 degree winds, and then shifting to a clockwise rotation with 250 degree winds; see Figure 9 which is a magnified picture of the northeast corner of Figure 7. Also computational results suggest that with increasingly westerly winds, the long tail of the recirculation, rather than flowing parallel to the tree line, penetrates the trees moving east.

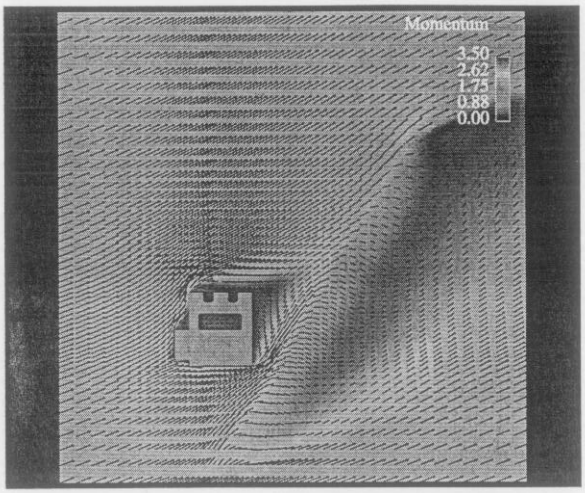

Figure 5. Velocity vectors and contours of momentum on a plane 2.6 meters above the ground. Wind direction: 225 degrees.

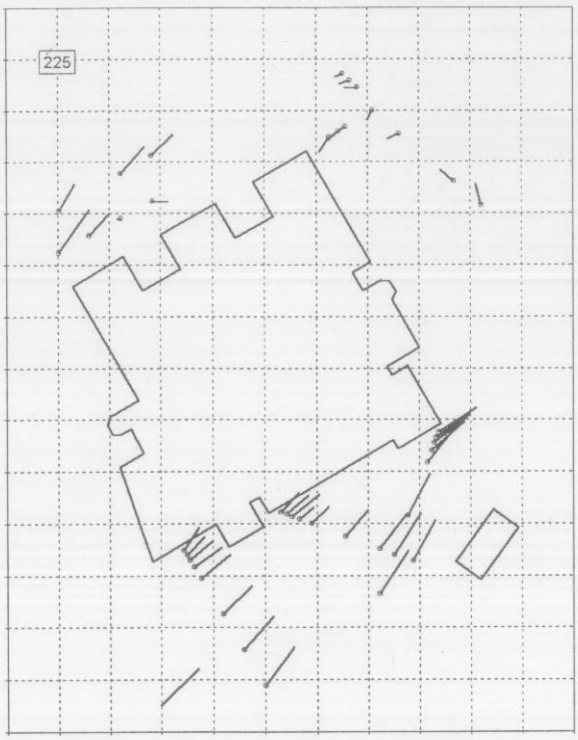

Figure 6. Experimental winds for 225 degrees. Tail of vectors indicated by circles.

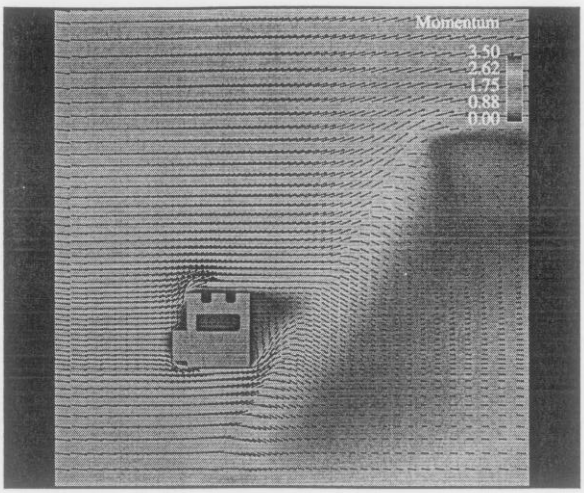

Figure 7. Velocity vectors and contours of momentum on a plane 2.6 meters above the ground. Wind direction: 250 degrees.

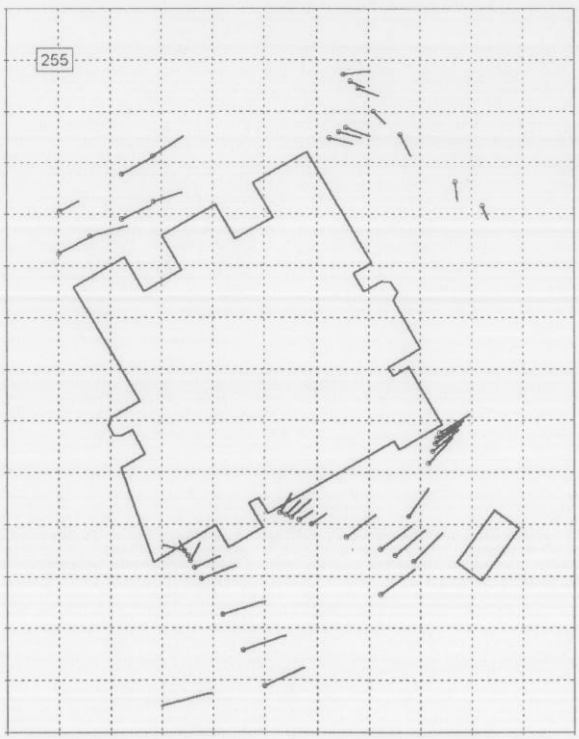

Figure 8. Experimental winds for 255 degrees. Tail of vectors indicated by circles.

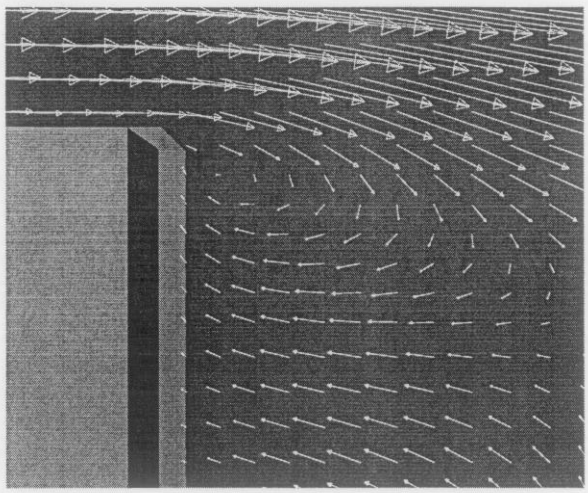

Figure 9. Magnified view of northeast corner of Figure 7.

4.2 Effect of the trees

Detailed experimental measurements in the tree area are not available at the time of this writing, but model predictions and experimental data agree that a major effect of the trees is to cause a channeling of winds around the southeast corner of the building. Model results predicted and the field experiment found a higher than ambient jet near this corner.

In the 200 degree case, model predictions show the momentum of the flow is dramatically reduced by the effect of the trees. As can be seen by comparing the relative size of the low momentum areas, the trees affect the overall flow field much more than the building. When the winds more directly oppose the tree line (cases 225 and 250), a stronger sheltering effect can be seen to the east.

4.3 Courtyard flow pattern

At the time of this writing, data is being collected in the courtyard of B170 and not available yet for comparison. Model predictions are given below. Velocity vectors and traces in the courtyard for the 200 degree case show that flow is similar to a lid driven cavity with the addition of a secondary spiral of air toward the northeast corner of the courtyard (see Figure 10).

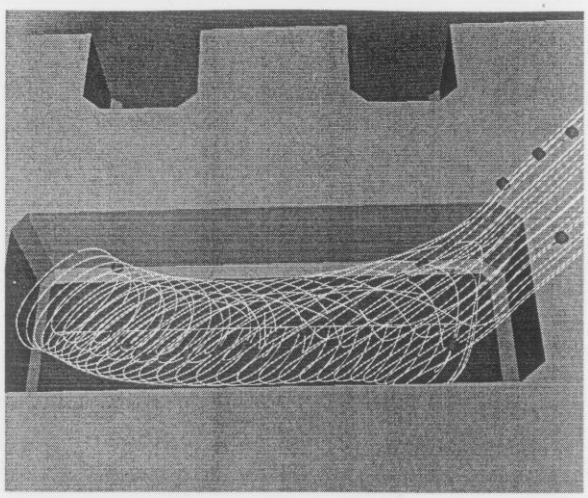

Figure 10. Traces released from a horizontal line source in the courtyard (2 meters above the ground). Wind direction: 200 degrees.

The 225 degree case shows a similar but more skewed (westerly) pattern in the courtyard. In the 250 degree case, little spiraling is apparent.

Model results suggest that air upstream of the building near the ground is more likely to enter the courtyard when the direction of the wind is more in line with the longer axis of the courtyard. For example in the 225 case, 2 meter air may enter, and in the 250 case 1 meter air may enter the courtyard.

4.4 Flow in alcoves and sides

Flow in the alcoves is similar for wind directions 200 and 225. Flow moves into the northern alcoves at the 2.6 meter height and out at 9.6 meters; see Figures 11 and 12. However in the 250 case, the major flow pattern in the alcoves below the immediate level of the roof is clockwise looking down (see Figure 13). Results from the field experiment for the flow in the alcoves will soon be available.

For all three wind directions, a weak southerly flow is present along the northeast face of the building (at the 2.6m height). Flow near the north face of the building moves west for the lower degree wind directions and then switches to moving east when the winds are more from the west (250 degrees). For prevailing winds, the flow along the southern face is generally toward the east with the exception of the beginnings of a recirculation near the southwest corner of the building when the winds are strongly from the west. Along the western face of the building, air moves toward the north for wind directions below about 245 degrees. Beyond 245 degrees, the air along the northern part of this face moves north and the air near the southern part of the face moves south.

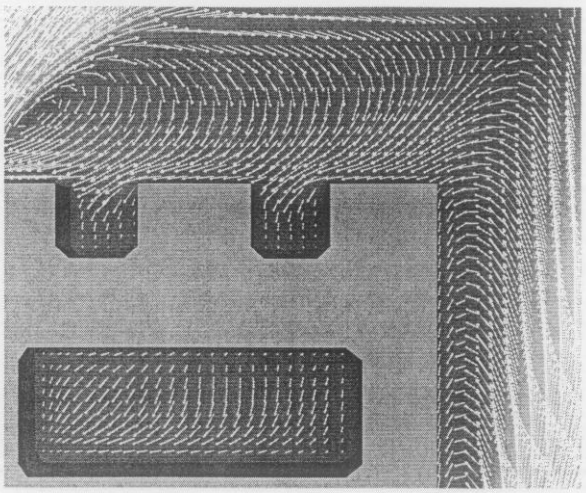

Figure 11. Velocity vectors in alcoves at 2.6 meter height. Wind direction: 200 degrees.

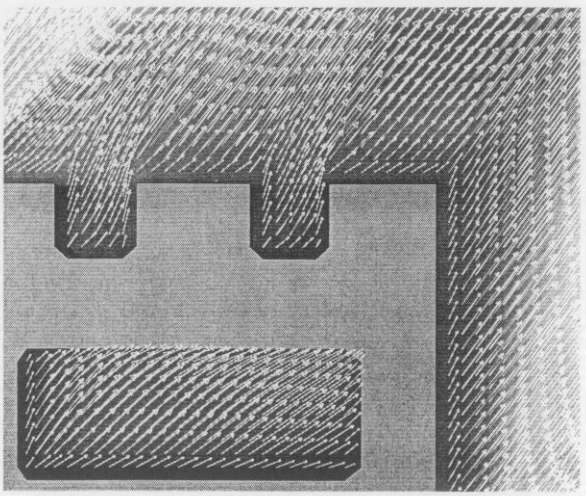

Figure 12. Velocity vectors in alcoves at 9.6 meter height. Wind direction: 200 degrees.

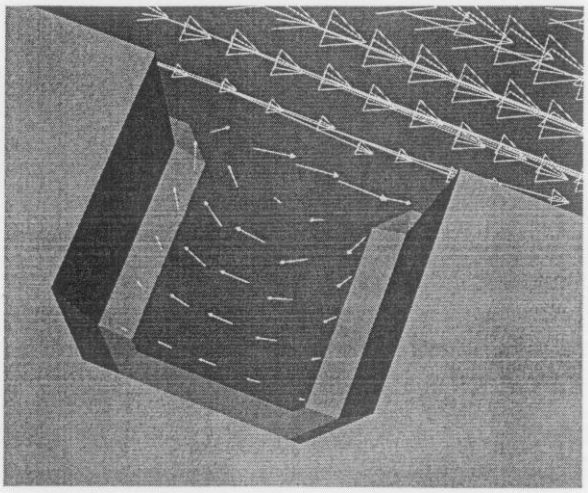

Figure 13. Vectors in alcoves at 2 m height. Wind direction: 250 degrees.

5. SUMMARY

Predictions for the flow pattern around a single complex building were produced in advance of a field experiment. Model results predict that the row of eucalyptus trees plays an important role in the flow pattern for the prevailing winds observed in the summer. In addition to slowing the flow in the area around the canopy, a region of higher velocities forms between the southeast corner of the building and the trees.

Mean recirculations form in the lee of the building. A mean clockwise vortical motion exists near the northern face of the building, and a mean eddy rotates counterclockwise near the eastern face (for 200 and 225 degree winds on a 2.6 meter high horizontal plane). As winds shift toward the west, the recirculation zone on the northern face flattens and finally disappears for winds coming from 250 degrees. Simultaneously, the recirculation near the east and northern corner of the building reverses direction and rotates clockwise.

In the 200 degree case, air parcels leaving the recirculation zone follow west and parallel to the tree line. However in more westerly winds, air parcels leaving the recirculation may penetrate the tree line.

Air movement in the courtyard is lid driven cavity-like with a secondary spiraling of the motion toward and exiting the east side of the courtyard. In the 200 and 225 cases, the spiraling motion is relatively strong compared to the 250 case where little spiraling motion is apparent. In all three cases, air exits the courtyard primarily near the northeast face.

As the winds become more westerly, air movement in the alcoves on the northwest side of the building changes from a predominantly up-down circulation of air to to a clockwise horizontal circulation.

Available field data suggest that model predictions were fairly accurate in prediction of important flow characteristics; for example, the higher than ambient jet, and the locations and shifts in directions of the recirculation zones. Additional comparisons for the alcoves, the courtyard, and the canopy region will soon be available. The dispersion segment of the field experiment is in the planning stages.

Acknowledgment

Special thanks are due to Frank Gouevia who provided key insights and support for the field experiments.

This work was performed under the auspices of the U.S. Department of Energy by Lawrence Livermore National Laboratory under contract no. W-7405-ENG-48.

BIBLIOGRAPHY

Gresho, P., and Chan, S. 1998, Projection 2 goes turbulent - and fully implicit. *Int. J. Comp. Fluid Dyn.* **9**, 249-272.

Chan, S. 1994, An improved three-dimensional heavy-gas dispersion model: User's Manual. *UCRL-MA-116567 Rev. 1.* **Lawrence Livermore National Laboratory.**

Arya, S. 1988, Introduction of Micrometeorology. *Academic Press.* **San Diego.**

Stevens, D., Almgren, A., Bell, J., Beckner, V., and Rendleman, C. 1999, Small scale processes and entrainment in a stratocumulus marine boundary layer. *J. of the Atmos. Sci..* **In Press.**